CONTROLLING ELECTROMAGNETIC VIBRATING FEEDER BY USING A MODEL PREDICTIVE CONTROL ALGORITHM

Petar Misljen[1*], Marko Tanaskovic[2], Zeljko Despotovic[3], Milan Matijevic[1]

[1]Faculty of engineering, University of Kragujevac, Kragujevac, Serbia

[2]Electrical engineering and computing, Singidunum University, Belgrade, Serbia

[3]Institute "Mihailo Pupin", University of Belgrade, Belgrade, Serbia

*petarmisljen@gmail.com

This paper examines the practical application of Model Predictive Control (MPC) algorithm for vibrating feeder with an electromagnetic actuator. In the base of this practical application are two microcontrollers STM32F407, one for digital data acquisition and implementation of the signal envelope detection and the other for implementation of the controller algorithms. Linearization of the well-known nonlinear system model and discretization of adopted linear system model has been performed. The linearized model has been experimentally verified. It has been proposed an algorithm for the envelope detection of the trough movement signal. This algorithm is made for concrete application in vibratory feeders, but its principle of operation is practically applicable for all the low dynamic processes. A comparison has been made for the obtained experimental results of the system with the feedback for the MPC and the PI controller. The frequency characteristics of the system with feedback have been recorded and its stability has been confirmed.

Keywords: model predictive control; envelope detector; vibrating feeder; STM32F407

1. Introduction

The problem of vibrations is present in many areas and it is the subject of various studies. Electromagnetic vibratory feeders (EVF) have a wide range of application in the process industry for bulk materials (conveying, dosing, screening, etc.). An electromagnetic vibratory actuator (EVA) is used as an electromechanical driving device. The transport of bulk materials is done through the vibratory trough. The vertical component of vibratory acceleration acts on bulk materials and make micro-

throw of material particles [1,2]. Changes in the conveying rate of the material can be made by changing the vibration excitation frequency and dual vibration amplitude of the vibrating trough [3,4]. An EVA is an electromagnetic generator of a mechanical force. This force is proportional to the square of the EVA current. It is possible to control the frequency and duration of the electromagnetic force by changing the parameters of the excitation current. Under these conditions, the whole conveying system with an EVF can be treated as a controllable mechanical oscillator [5-8]. The use of elastic elements is justified because they allow for the creation of conveyors without the use of mechanical elements such as gears, cams belts, bearings, eccentrics or motors and makes electromagnetic vibratory conveyors and EVFs the most cost-effective equipment [7,8]. The springs are under the greatest stress in the upper and lower parts [9]. If an EVF operates in resonant mode, the desired material flow will be achieved with minimum energy consumption. The amplitude of oscillation is limited to the construction of the EVF and can be controlled by proper amplitude control. Since the resonant frequency depends on the stiffness of the spring and the quantity of material to be transported, it is necessary to find and monitor the right resonant frequency to achieve energy efficiency. This can be achieved with an appropriate amplitude-frequency control. In this way, the EVF achieves the minimum power consumption [5,6] and improves the input power factor of the regulated EVF operation [10]. A power factor correction (PFC) converter is included in the power converter of the EVF and it is in fact the pre-regulator that stabilizes the mains AC voltage 230V to 400 VDC. The cited references [5,7,8,11] discuss the structure of the controller for the EVA, the motion of a linear vibratory feeder and control algorithms based on the application of PID controllers. The cited references [5,7,8,11] discuss the structure of the controller for the EVA, the motion of a linear vibratory feeder and control algorithms based on the application of the PID controller. The main objectives of this paper are to determine the parameters of the predictive controller for the amplitude control of the trough vibrations, the simplification of the signal envelope detection and the realization of the signals acquisition system in the microcontroller environment. The accepted linearized model of the EVF has been implemented in Simulink / Matlab environment and Model Predictive Control (MPC) controller has been practically realized.

2. Accepted model of the EVF

A detailed description of a nonlinear model of an EVF is shown in the cited literature [12] and this model has been used in this paper.

The experimental setup, which is shown in Figure 1, includes the following instruments: (1) a multimeter; (2) an oscilloscope; (3) a DC power supply for sensors; (4) a control unit with an insulated-gate bipolar transistor (IGBT) converter; (5) digital scales; (6) an actuator and (7) an inlet hopper with shutter.

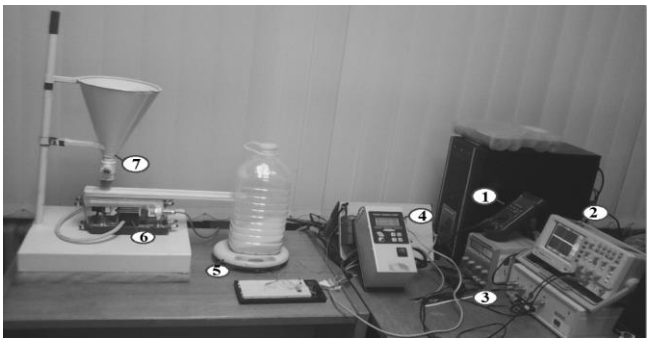

Figure 1. The experimental setup.

The change in the amplitude of the trough vibrations is done by changing the value of the parameter $A_p[\%]$. The value of this parameter is proportional to the energy that the energy converter transfers to the electromagnetic actuator. The value of the $A_p[\%]$ parameter can be changed manually by entering the value in the 0-100% range using the keypad, or by electronically changing the voltage level in the 0-10 V range at the appropriate input of the control unit.

The variable $p[m]$ represents a displacement of the trough moving in a horizontal plane. The EVA coil current is a periodic signal and it can be expanded in terms of a sinusoidal components.

The dependence of the mean value of the coil current from the $A_p[\%]$ parameter value has been experimentally determined as:

$$I_{SR} = 3A_P + 55[mA], \forall A_P > 0$$
$$I_{SR} = 0, \forall A_P = 0 \quad (1)$$

The coli current (i) can be represented as the triangle pulse array with amplitude Am and its time distances of T/4, where T is the period of the pulse repetition. In the time domain, the coil current is a periodic function that can be developed into a Fourier series:

$$i(t) = a_0 + \sum_{k=1}^{\infty} a_k \cos k\omega t \quad (2)$$

$$a_0 = \frac{3A_m}{8} \quad (3)$$

$$a_k = \frac{8A_m}{3\pi^2 k^2}\left(1 - \cos\frac{k3\pi}{4}\right) \quad (4)$$

$$i(t) = \frac{3A_m}{8} + \sum_{k=1}^{\infty} \frac{8A_m}{3\pi^2 k^2}\left(1 - \cos\frac{k3\pi}{4}\right)\cos k\omega t \quad (5)$$

An acceptable approximation of this signal is obtained by presenting the signal with the null, basic and three higher harmonics:

$$a_1 = \frac{4A_m\left(2+\sqrt{2}\right)}{3\pi^2} \quad (6)$$

$$a_2 = \frac{2A_m}{3\pi^2} \quad (7)$$

$$a_3 = \frac{4A_m\left(2-\sqrt{2}\right)}{27\pi^2} \quad (8)$$

$$a_4 = \frac{A_m}{3\pi^2} \quad (9)$$

The null harmonic (a0) represents the mean value of the coil current. On the basis of equations (1) and (2), the dependence of the coil current amplitude from the parameter A_p[%] is:

$$A_m = 8A_P + \frac{8}{3}55[mA] \quad (10)$$

Filtering the signal p gives an envelope which contains information about the oscillation amplitude of the vibrating trough in the horizontal plane (P).

One way to extract the envelope signal is based on the Hilbert's transformation of the signal p. After Hilbert transformation of the signal p there are obtained sinusoidal signals P_l and P_q. These signals are phase-shifted by 90 degrees each other and they have amplitudes which are equal to the amplitude of signal p.

$$P_l = \frac{(s-374800)(s-48000)(s-11270)(s-2620)(s-623)(s-134.9163)}{(s+374800)(s+48000)(s+11270)(s+2620)(s+623)(s+134.9163)}\,p \quad (11)$$

$$P_q = \frac{(s-107410)(s-23400)(s-5446.6)(s-1279.75)(s-300.03)(s-38.38)}{(s+107410)(s+23400)(s+5446.6)(s+1279.75)(s+300.03)(s+38.38)}\,p \quad (12)$$

Envelope P_h of the signal p at the output of the detector is:

$$P_h = \sqrt{P_l^2 + P_q^2} \quad (13)$$

The Bode's diagrams of the filter that performs the Hilbert transform are shown in Figure 2. This filter has a single amplification (0 dB) and on its outputs two signals that are phase-displaced by 90 degrees in the frequency range of interest (250 - 750 rad/s).

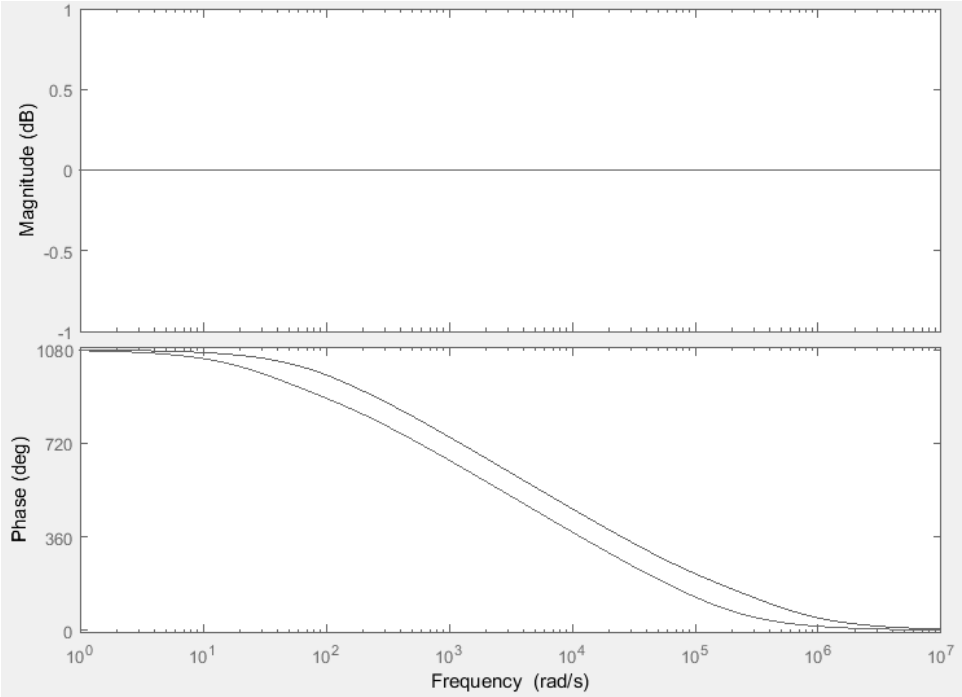

Figure 2. The Hilbert transform. Bode's diagram.

Since the Hilbert's transformation does the phase shift of the signal by approximately 90°, the signal on the filter outputs also contains a sinusoidal component whose frequency is equal to the frequency of the trough oscillation. This "high frequency" component is suppressed using a Butterworth filter with the following transfer function:

$$H_b(s) = \frac{1}{\prod_{k=1}^{n}(s - s_k)/\omega_c}, s_k = \omega_c e^{\frac{j(2k+n-1)\pi}{2n}} \quad (14)$$

with the transferring function of the low frequency filter $P(s) = H_b(s)P_h(s)$.

In the concrete case it was accepted that it is $n = 8$ and $\omega_c = 188 rad/\sec$, where n and ωc are the order and the boundary frequency of the filter, respectively.

3. The control structures

The application of the MPC controller implies the existence of a linear discrete system for which are known all the limitations of input, measured and output variables. In the view of the aforementioned non-linearity of the observed system, and for the purpose of applying the MPC controller, it is necessary to select the operating point of the system, perform the linearization of the system around the selected operating point and to discretize the adopted linear system model.

3.1. Identification and linearization

Equations (1) - (14) represent a mathematical apparatus which is the starting point for the simulation of the vibrating trough work. However, the application of this device in some experimental environment requires significant capacities in the form of processor power and memory size.

In order to simplify and adapt this mathematical apparatus to the application in the experimental environment, there is recorded the dependence of the vibration amplitude of the trough (P) from the parameter $A_p[\%]$. The diagram was recorded for coil current whose frequency is equal to the mechanical resonance frequency of the EVF (fmr = 50.3 Hz). The obtained values are shown in Figure 3.

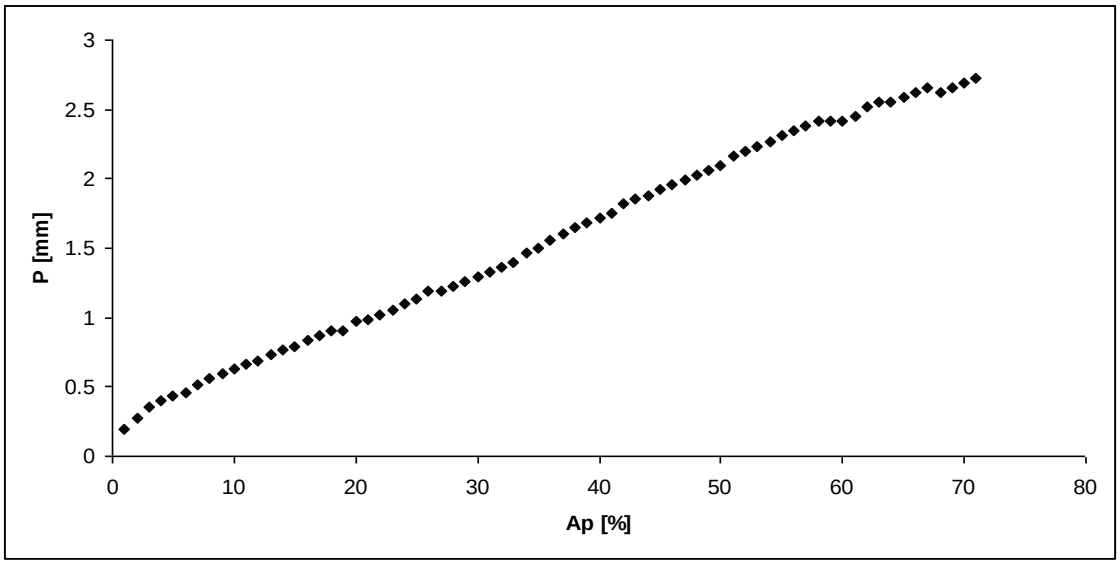

Figure 3. The dependence of the vibration amplitude of the trough (P) from the value of parameter $A_p[\%]$, fmr = 50.3 Hz.

The EVF transmission response to the impulse force acting on the trough carrier is shown in Figure 4. The response shown in Figure 4 has been obtained by simulation, and his time constant is identical to the time constant of the response obtained in the experimental conditions. The response obtained in the experimental conditions is shown in Figure 5. The impulse force has been simulated by the pulse of the unit size with the duration period of 0.001 seconds. In experimental conditions, it is obtained by short-term, instantaneous, action of force on the trough carrier. This response is crucial for identifying the dynamics of the vibrating conveyor as a whole.

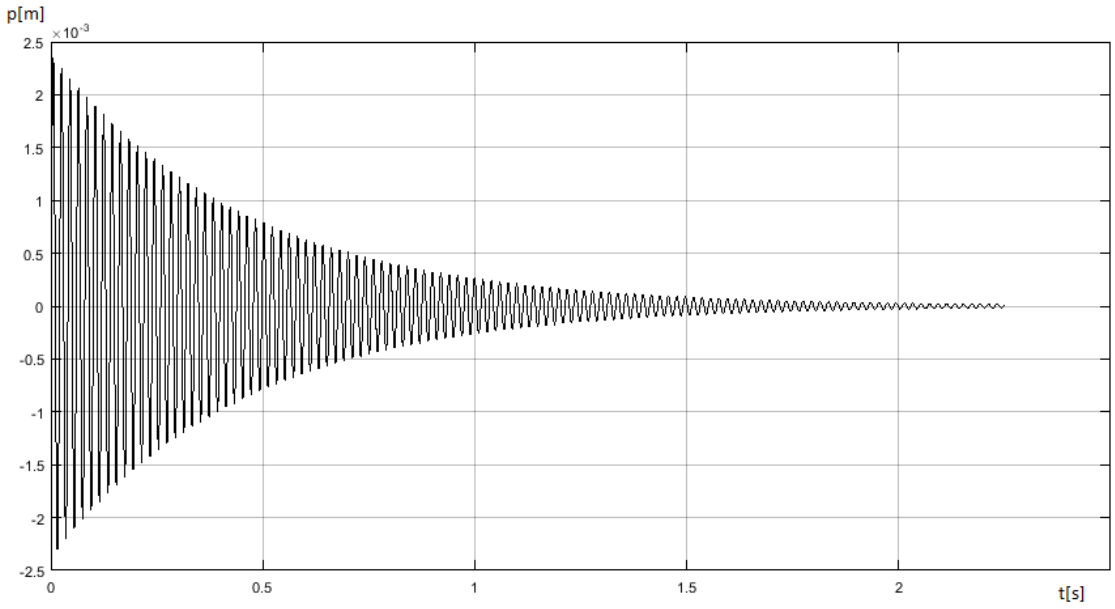

Figure 4. The EVF transmission response to the impulse force acting on the trough carrier, simulation.

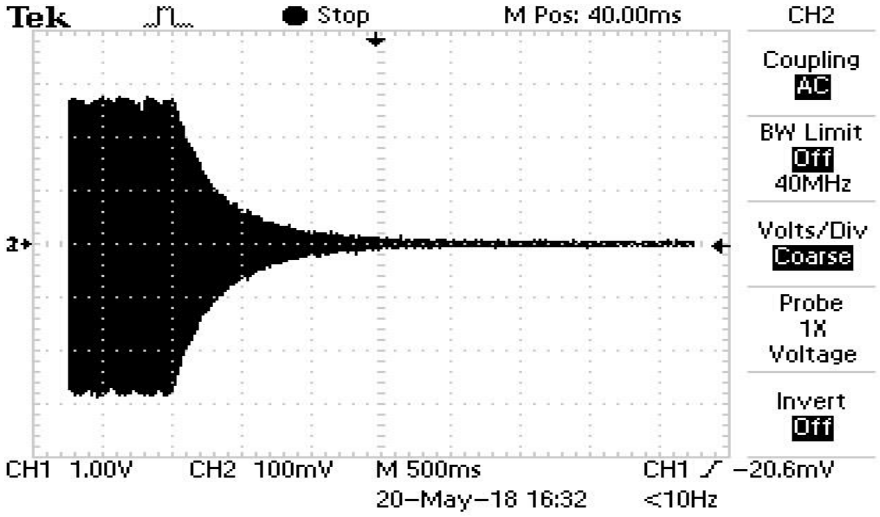

Figure 5. The EVF transmission response to the impulse force acting on the trough carrier, experiment.

Based on the diagram shown in Figure 3, the dependence of the vibration amplitude of the trough from the parameter $A_p[\%]$ can be written in the following form for a stationary state:

$$P = 3.671e-5 \cdot A_p + 2.622e-4[m] \qquad (15)$$

Starting from the equations (1) - (14), a simulation was initiated and parametric identification was performed in order to determine the direct dependence between parameters $A_p[\%]$ and P . The following transfer function was obtained:

$$\frac{P}{A_P + A_0} = \frac{K}{1 + T \cdot s} \tag{16}$$

where K = 6.671e-5, T = 0,4442, A0= 7.142468%.

In order to apply the MPC controller, it is extremely important to define which constraints exist in the system. The flow of material through the trough cannot be higher than the input of the material from the receiving hopper. The maximum value of material flow through the trough is determined by the position of the shutter on the receiving hopper and it is considered as constant. The trough vibration amplitude is limited by the width of the electromagnet air gap. The literature [12] defines the conditions for the energy efficiency of the electromagnetic vibratory feeder. The critical value of the trough vibration (P_{cr}) has been determined. Increase of the trough vibration amplitude over P_{cr} wouldn't increase the speed of the bulk material through the trough, but the level of material in the trough would be reduced. If the trough vibration amplitude is less than its critical value, it was shown that the adopted model corresponds to the nonlinear system and that the adopted simplifications of the nonlinear model do not have a significant influence on the accuracy of the adopted model. From the point of view of the application of the MPC controller, keeping the trough vibration amplitude below the critical value is of particular importance because in that case there is no change in the total mass loaded on the EVF springs, and consequently there is no change in the mathematical model of the EVF.

3.2. Hardware environment

Two microcontrollers STM32F407VGT6 are used. One for processing the signals from the trough displacement sensor and another for generating the control variables. The STM32F4 board used in this work is shown in Figure 6.

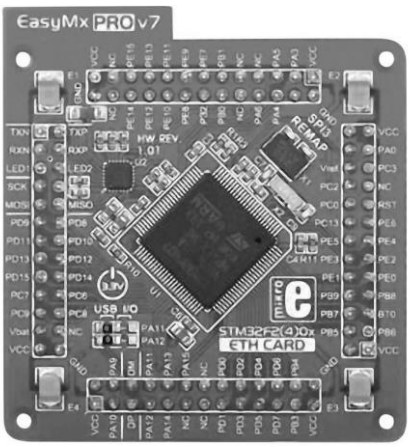

Figure 6. Microcontroller board with STM32F407VGT6 (manufactured by Mikroelektronika, Belgrade).

Microcontroller STM32F407VGT6 is developed for educational purposes and belongs to the STM32F4 series of microcontrollers. The STM32F4 series microcontrollers are used in a wide range of devices, from battery control to real-time aircraft management. The components of this series of microcontrollers have affordable price and allow the use of various software tools. On the board shown in Figure 6, the ARM Cortex-M4 core is installed, which can operate at clock speeds up to 168 MHz. The STM32F4 series is compatible with all ARM tools and programs. A block diagram of controlling the EVF trough vibration amplitude is shown in Figure 7.

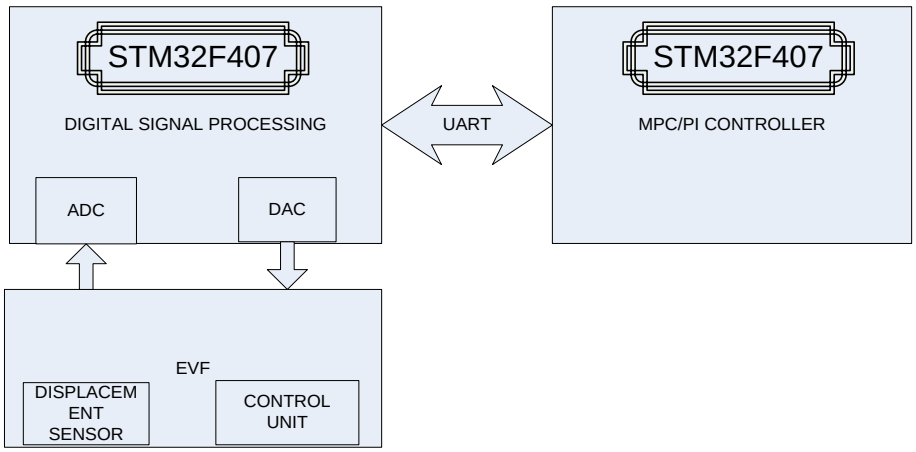

Figure7. A block diagram of controlling the EVF trough vibration amplitude.

To set parameters of the microcontroller periphery, the STM32CubeMX graphic software, with the Keil toolchain, has been used. This software initializes the program code written in the C programming language. The exchange of data between the digital signal processing board and the board for generating the control variable is realized through a serial connection based on the UART protocol. The output of the DA converter on the digital signal processing board is connected to the input for the control signal on the control unit of the EVF.

3.3. The envelope detection

The parameter A_p[%] is defined as the control variable. The EVF trough vibration amplitude has been defined as measurable variable. Setting the parameter A_p[%] values is done by changing the corresponding voltage level in the range 0-10 V, which corresponds to the change of parameter A_p[%] in the range 0-100%.

The signal at the output of the displacement sensor is a periodic signal that has a sine wave shape in the operating point.

One AD converter and one DA converter have been activated on the digital signal processing board. The signal from the displacement sensor is connected to the input of the AD converter and its sampling is performed with a sampling time of 500 μs. Based on 39 samples, the mean value of the signal from the displacement sensor is calculated.

By subtracting the mean value of the signal from its current value, an alternating component of the signal is obtained, which represents the movement of the EVF trough. The envelope of this signal presents information about the movement of the EVF trough in horizontally plane. The current value of the envelope is sent to the controller board to generate the control variable. On this board, the applied controller algorithm (MPC or PI) is executed and the calculated value of the control variable is returned to the microcontroller on the digital signal processing board. This microcontroller performs DA conversion and sends the control signal to the control unit of the vibratory conveyor.

The timing diagram of the signal envelope is shown in Figure 8. Before filtering the signal envelope, the negative part of the signal has been cut off due to the noise elimination.

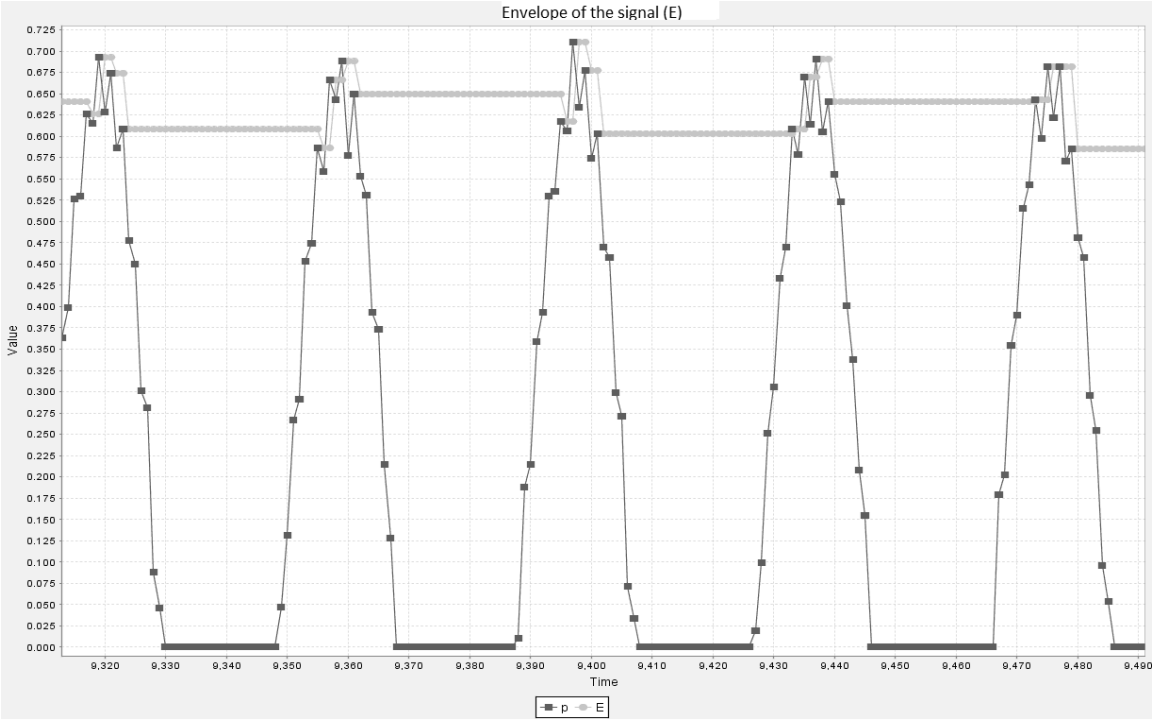

Figure 8. Envelope of the trough movement signal.

The most commonly used envelope detection methods are the Diode AM detector and the Synchronous AM detector.

Diode AM detector is by far the simplest form of AM demodulator or detector, requiring just a semiconductor (or other form) of a diode along with a capacitor to remove high frequency components. It suffers from a number of disadvantages, but its performance is more than adequate for most applications including broadcast receivers where cost is a significant driver.

The synchronous form of AM detector offers a higher level of performance, but with significantly more components. This means that it is only used in receivers where the performance levels are paramount and can justify the additional component costs.

In order to avoid the disadvantages of the diode detector and the high cost of the Hilbert transformation detector, the signal from the displacement sensor is processed using a microprocessor. STM32F407 microcontroller is available with a relatively low cost. The applied method of the envelope detecting, i.e. the peak detection, is based on calculating the difference in the values of the successive signal samples and finding the sample after which this difference changes its the sign from the positive to the negative.

Let $\Delta(k) = p(k) - p(k-1)$ be a difference in the value of successive samples. Then, the peak is detected at the moment k if and only if: Δ (k-1)> 0 and Δ (k) <= 0. In that case the envelope of the signal at time k (E (k)) is determined according to the algorithm shown in Figure 9.

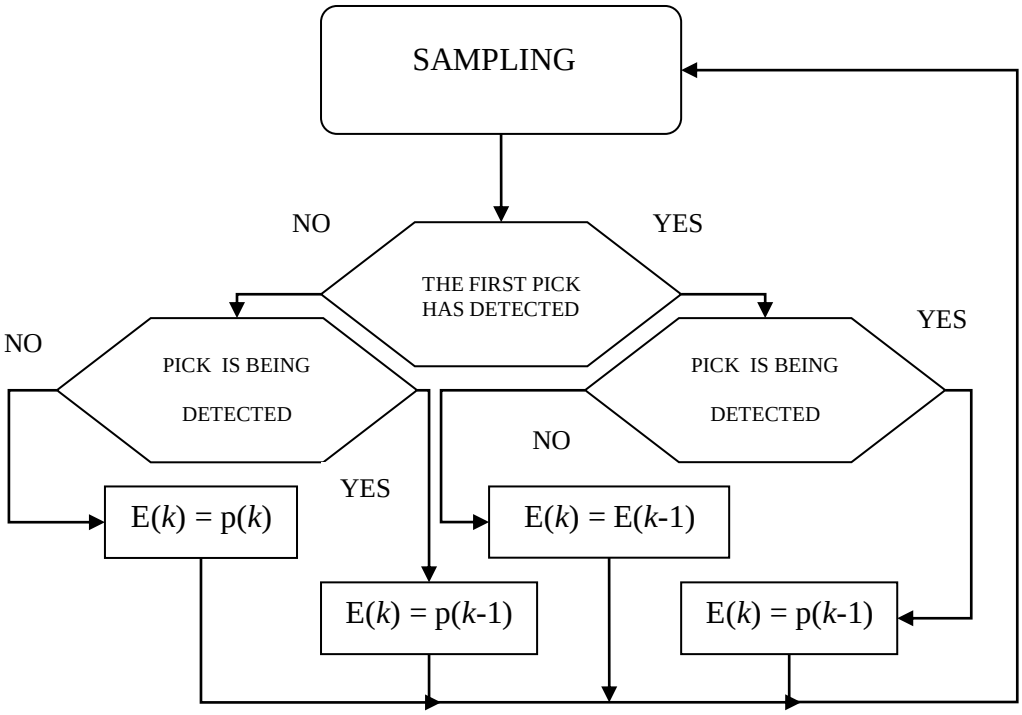

Figure 9. Algorithm for envelope detection.

3.4. The control variable generating

In order to generate the control variables two algorithms were considered, MPC and PI controller. The MPC controller is a predictive controller that minimizes the criteria function. An example of the application of the MPC controller in the environment of the microcontroller STM32F407 is shown in the cited literature (13). Let the discrete model in the state space is in the following form:

$$\Delta x(k+1) = A\Delta x(k) + B\Delta u(k),$$
$$\Delta y(k) = C\Delta x(k) \tag{17}$$

where $\Delta x(k) \in R^{np}$ is the vector of the system state change, $\Delta u(k) \in R^{n}$ is the input change vector and $\Delta y(k) \in R^{p}$ is the change of the measurable outputs. The Δ operator provides the elimination of a static error, while the A, B, C and D are matrices of the corresponding dimensions. Based on the equations (17) the change of in the system state at the moment $k + j$:

$$\Delta x(k+j \mid k) = A^{j}\Delta x(k) + \sum_{i=1}^{j} A^{j-i} B\Delta u(k+i-1) \tag{18}$$

By involving the equation (18) to the equation (17), the output of the predictor is obtained, i.e. the values of the output of the system at the moment $k + j$ are predicted based on the knowledge of the system state at the moment k:

$$\hat{y}(k+j \mid k) = y(k) + \sum_{i=1}^{j} CA^{i}\Delta x(k) + \sum_{i=1}^{j}\sum_{l=0}^{j-i} CA^{l} B\Delta u(k+i-1) \tag{19}$$

The MPC controller based on this the state space model of the system should minimize the criteria function presented in the following square form:

$$J = \sum_{j=1}^{H_p}\left(\hat{y}(k+j \mid k) - w(k+j)\right)^{2} + \lambda\sum_{i=1}^{H_c}\Delta u(k+i-1)^{2} \tag{20}$$

where H_p is the system output prediction horizon, H_c represents the calculation horizon of the control variable value, λ represents the weight coefficient for evaluating the square of the input variable change in the criterion function, w(k + j) represents the desired output value at the moment $k + j$ and $\hat{y}(k+j \mid k), j \in [1, H_p]$ is presented in the equation (19). Because of simplify of the mathematical apparatus it has been transformed into the matrix form. The output values corresponding to the defined horizon H_p are presented as follows:

$$Y = L\Delta U + f \tag{21}$$

where:

$$Y = [\hat{y}(k+1 \mid k), \hat{y}(k+2 \mid k), \ldots, \hat{y}(k+H_p \mid k)]^{T},$$
$$\Delta U = [\Delta u(k), \Delta u(k+1), \ldots, \Delta u(k+H_c - 1)]^{T}.$$

It was assumed that there was no change in the control variable after the moment $k + H_c - 1$, i.e. $\Delta u(k+1) = 0$ for $i > H_c - 1$. Although the MPC controller performs a calculation for changing the control variable for the H_c horizon, only the value referring to the moment k, i.e. $\Delta u(k)$, is transmitted to the plant. The desired output values are represented by a matrix W, where:

$$W = [w(k+1), \ldots, w(k+H_p)]^{T}. \tag{22}$$

Based on the equations (17) - (22), the following matrices have been defined:

$$f = \begin{bmatrix} y(k) \\ \vdots \\ \vdots \\ \vdots \\ y(k) \end{bmatrix} + F\Delta x(k) \tag{23}$$

$$F = \begin{bmatrix} CA \\ CA + CA^2 \\ CA + CA^2 + CA^3 \\ \vdots \\ \sum_{i=1}^{H_p} CA^i \end{bmatrix}, \; L = \begin{bmatrix} CB & 0 & \cdots & 0 \\ CB + CAB & CB & 0 & 0 \\ CB + CAB + CA^2B & CB + CAB & \ddots & \vdots \\ \vdots & \vdots & \ddots & \vdots \\ \sum_{j=1}^{H_p} CA^{j-1}B & \cdots & \cdots & \sum_{j=1}^{H_p - H_c} CA^{j-1}B \end{bmatrix}$$

where $L \in R^{pH_p xnH_c}$ and $f \in R^{pH_p x1}$.

Now, the criterion function (20) can be represented in the matrix form:

$$J = (Y - W)^T (Y - W) + \lambda \Delta U^T \Delta U \tag{24}$$

By minimizing the equation (24) by the value of ΔU, it has been obtained:

$$\Delta U = \left[L^T L + \lambda I_{H_C} \right]^{-1} L^T [W - f] \tag{25}$$

where $I_{H_c} \in R^{H_c xH_c}$ the unit matrix.

On the basis of equation (25) it is possible to define the first element of the vector ΔU. Now the control variable can be calculated as:

$$u = u(k-1) + \tilde{L}(W - f) \tag{26}$$

where $\tilde{L}$ represents the first row of the matrix $\left(L^T L + \lambda I_{H_c} \right)^{-1} L^T$.

Equations (17) - (26) represent a mathematical apparatus that is applied to the realization of the MPC control structure based on microcontrollers.

The control variable of the PI controller is calculated according to the following:

$$u(k) = K_p e(k) + K_I \left(e(k) + \sum_{j=0}^{k-1} e(j) \right) \tag{27}$$

where $e(k) = w(k) - y(k)$ is the error signal, and the adopted PI controller parameters values are: $K_p = 1.265$ and $K_i = 2.531$. The tool from the Simulink environment was used to select the parameters of the PI controller.

The PI controller was considered with the sampling period $T_s = 0.1\text{sec}$ and the MPC controller with the sampling periods $T_s = 0.1\text{sec}$ and $T_s = 0.05\text{sec}$. The simulation responses of the EVF to the required value of the trough vibrating amplitude, for feedback with MPC, with a sampling period $T_s = 0.1\text{sec}$, is shown in Figure 10.

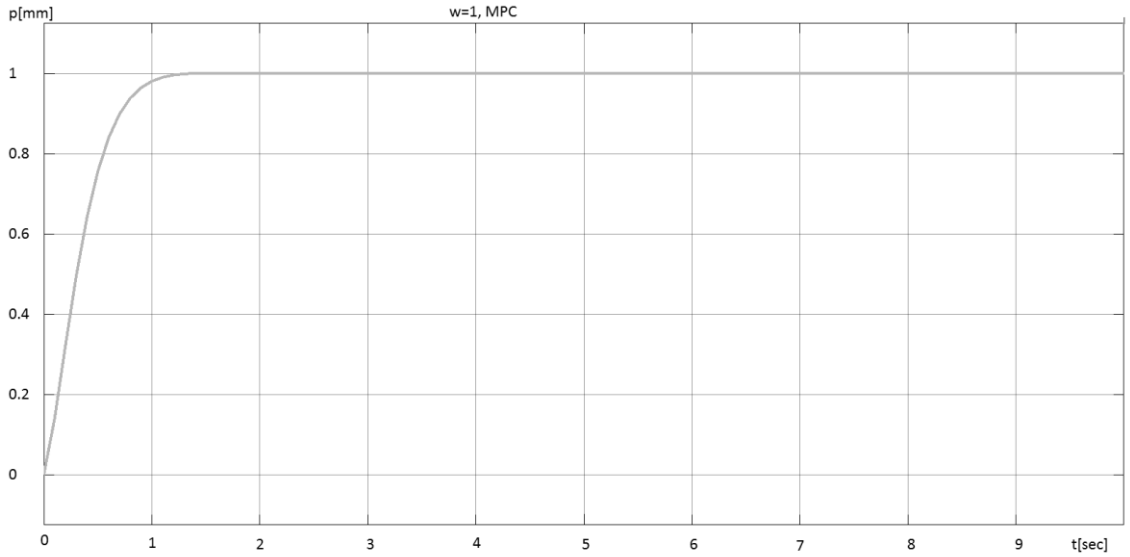

Figure 10. MPC controller, Ts = 0.1sec, simulation.

The experimental responses of the EVF to the required value of the trough vibrating amplitude, for feedback with MPC and PI controller, with a sampling period $T_s = 0.1\text{sec}$, are shown in Figure 11 and Figure 12, respectively.

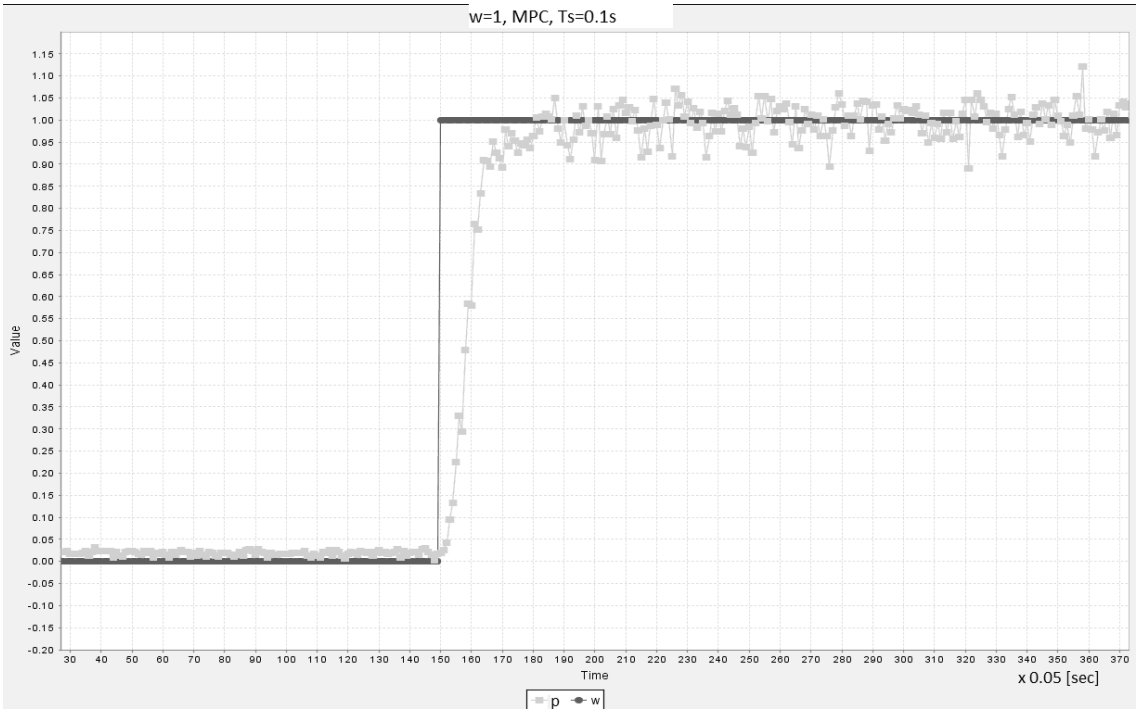

Figure 11. MPC controller, Ts = 0.1sec, experiment.

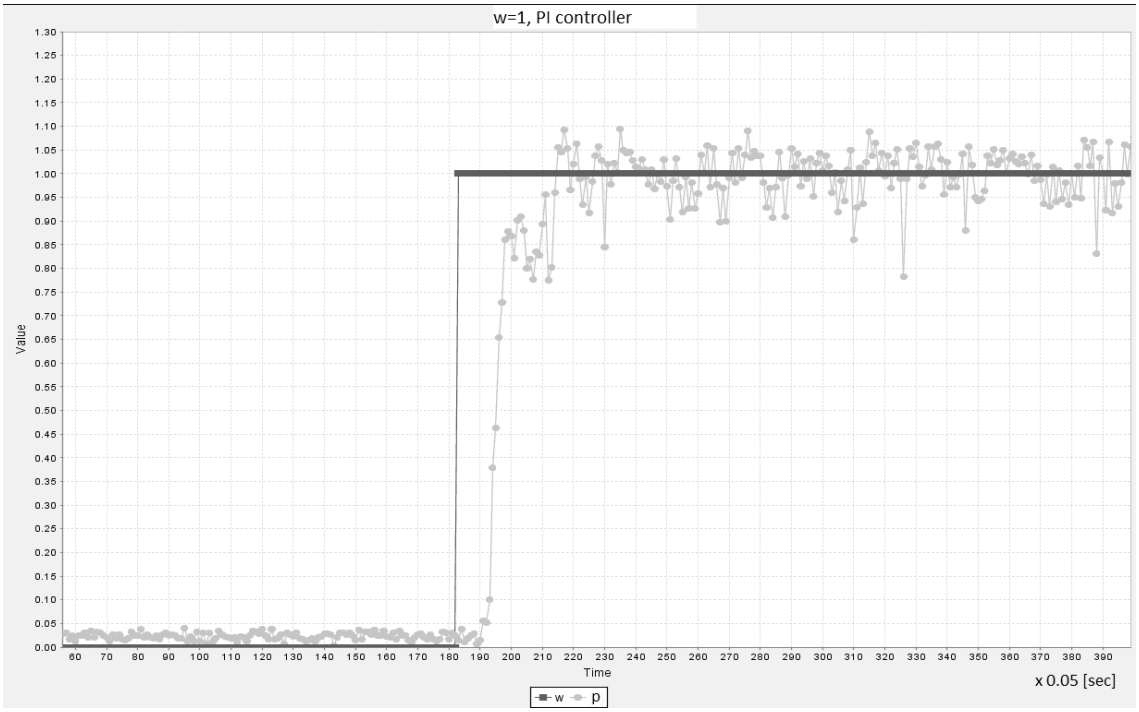

Figure 12. PI controller, Ts = 0.1sec, experiment.

Figures 11 and Figure 12 show that the applied MPC controller and the PI controller have a very similar response on the step excitation. In addition, an experimental verification of the simulation results shown in Figure 10 was completed.

For the purpose of comparing the frequency characteristics of the proposed controllers, the reference vibration amplitude values of the EVF trough were being changed in the form of sine functions with different frequencies. Responses were recorded for a frequency range of 0.01 Hz to 1 Hz, since the proposed controllers showed a high attenuation for a frequency greater than 1 Hz. On the basis of the obtained responses, the frequency diagrams were recorded and shown in Figure 13 and Figure 14. The ratio of the achieved (p) and the reference (w) amplitude of the trough amplitude were observed as the system amplification.

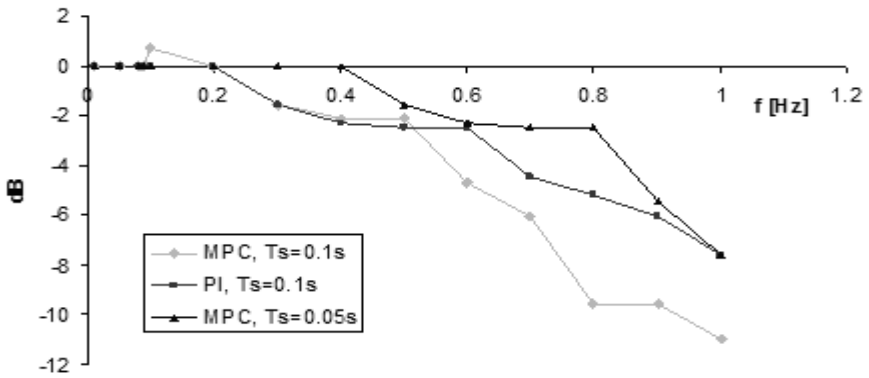

Figure 13. Amplitude-frequency characteristics.

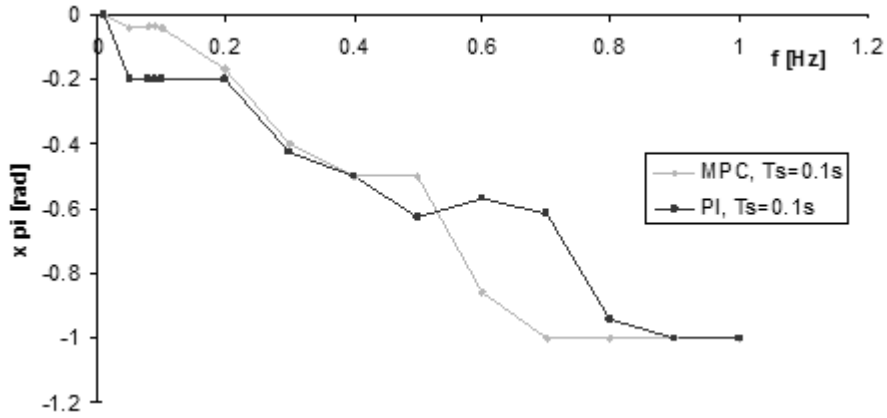

Figure 14. Phase-frequency characteristics.

4. Conclusion

If the bulk material's speed through the trough is less than critical, it is possible to successfully use the model predictive controller for controlling the EVF.

The bandwidth of the system with the PI controller is negligibly wider than the system with the MPC controller, so it can be concluded that the choice of the controller has no significant impact on the dynamic properties of the system.

Reducing the MPC controller sampling period increases the bandwidth of the closed-circuit system.

Based on the value of the frequency characteristics, it is obvious that the system with feedback keeps stability with both controllers.

The suggested algorithm for detecting the signal envelope gives satisfactory results for EVF and its principle of operation is practically applicable for all the low dynamic processes.

Further research in the development of control structures of vibration transport should be directed to the development of adaptive algorithms that will in real time monitor the changes in the dynamic parameters of the system in order to correct the parameters of the MPC controller.

References

[1] Han L, Tso SK. Mechatronic design of a flexible vibratory feeding system. Proceedings of the Institution of Mechanical Engineers, Part B: Journal of Engineering Manufacture. 2003; 217(6): 837-842.

[2] Sloot EM, Kruyt NP. Theoretical and experimental study of the transport of granular materials by inclined vibratory conveyors. Powder Technology. 1996; 87(3): 203-210.

[3] Parameswaran MA, Ganapahy S. Vibratory Conveying-Analysis and Design: A Review. Mechanism and Machine Theory. 1979; 14(2): 89-97.

[4] McGlinchey D. Vibratory Conveying Under Extreme Conditions: An Experimental Study. Advanced in Dry Processing 2002, Powder/Bulk Solids. 2001; 1: 63-67.

[5] Doi T, Yoshida K, Tamai Y, et al. Modelling and feedback control for vibratory feeder of electromagnetic type. Journal of Robotics and Mechatronics. 1999; 11(5): 563-572.

[6] Despotovic Z, Stojiljkovic Z. Power converter control circuits for two-mass vibratory conveying system with electromagnetic drive: Simulations and experimental results. IEEE Trans. Ind. Electron. 2007; 54(1): 453-466.

[7] Ribic AI, Despotovic Z. High-Performance Feedback Control of Electromagnetic Vibratory Feeder. IEEE Transaction on Industrial Electronics. 2010; 57(9): 3087-3094.

[8] Despotović ŽV, Ribić AI, Sinik V. Power Current Control of a Resonant Vibratory Conveyor Having Electromagnetic Drive. Journal of Power Electronics. 2012; 12(4): 678-689.

[9] Vujović M, Despotović Ž. Dynamic Stress Distribution in Composite Leaf Springs for Electromagnetic Vibratory Feeder. In: 3rd International Conference & Workshop Mechatronics in Practice and Education (MECHEDU); 14-16 May 2015; Subotica, Serbia.

[10] Despotovic ZV, Lecic M, Jovic M, et al. Vibration control of resonant vibratory feeder with electromagnetic excitation. Journal FME Transactions. 2014; 42(4): 281-289.

[11] Despotovic Z, Urukalo Dj, Lecic M, et al. Mathematical modelling of resonant linear vibratory conveyor with electromagnetic excitation: simulations and experimental results. Applied Mathematical Modeling. 2017; 41(1): 1-24.

[12] Misljen P, Despotovic Z, Matijevic M. Modeling and Control of Bulk Material Flow on the Electromagnetic Vibratory Feeder. AUTOMATIKA – Journal for Control, Measurement, Electronics, Computing and Communications. 2016; 57(4): 936-937.

[13] Rihab K, Hichem S, Faouzi B. Application of Model Predictive Control for a thermal process using STM32 Microcontroller. In: International Conference on Control, Automation and Diagnosis (ICCAD); 19-21 January 2017; Hammamet, Tunisia.